Hindawi
International Journal of Chemical Engineering
Volume 2019, Article ID 2531027, 8 pages
https://doi.org/10.1155/2019/2531027

Research Article

Influence of Sintering Temperature on Mechanical Properties of Glass-Ceramics Produced with Windshield Waste

Hiasmim R. Gualberto,[1] Ronie S. Lopes,[2] Fernanda A. N. G. da Silva,[3] Etyene Schnurr,[4] Edgard Poiate Junior,[5] and Mônica C. de Andrade[1]

[1]*Instituto Politécnico/Universidade do Estado do Rio de Janeiro (IPRJ/UERJ), Rua Bonfim, 25, IPRJ, Bloco 1, 1° andar, Sala 114, Vila Amélia, Nova Friburgo, RJ 28625-570, Brazil*
[2]*Centro Federal de Educação Tecnológica Celso Suckow da Fonseca (CEFET-RJ), Av. Governador Roberto Silveira, 1900, Prado, Nova Friburgo, RJ 28635-000, Brazil*
[3]*Instituto de Química/Universidade Federal do Rio de Janeiro (IQ/UFRJ), Av. Athos da Silveira Ramos, 149, Centro de Tecnologia, Bloco A, 6° andar, Sala 630, Ilha da Cidade Universitária, Rio de Janeiro, RJ 21941-909, Brazil*
[4]*Universidade Federal Fluminense Instituto de Saúde de Nova Friburgo, Faculdade de Odontologia, Rua Silvio Henrique Braune, 22 Centro, Nova Friburgo, RJ 28625-650, Brazil*
[5]*Instituto Politécnico/Universidade do Estado do Rio de Janeiro (IPRJ/UERJ), Rua Bonfim, 25, IPRJ, Bloco 1, 1° andar, Sala 215, Vila Amélia, Nova Friburgo, RJ 28625-570, Brazil*

Correspondence should be addressed to Mônica C. de Andrade; monicacalixtoandrade@gmail.com

Received 18 November 2018; Revised 27 January 2019; Accepted 5 February 2019; Published 1 April 2019

Academic Editor: Gianluca Di Profio

In this work, glass-ceramics were produced with mechanical and physical properties, using recycled glass powder from windshields as raw material. The glass powder was formed and sintered at temperatures 600, 650, 700, 750, and 800°C. Pieces were also produced with the addition of niobium oxide to the glass powder. The flexural strength and the Archimedes density of the produced parts were determined. The reliability of the results was evaluated by the Weibull statistic. X-ray diffraction was performed. Maximum flexural strength was 77.64 MPa at 750°C, with the addition of niobium oxide at 43.86 MPa at 700°C. X-ray diffraction showed crystalline structures in the specimens with the addition of the nucleating agent, confirming the production of glass-ceramics in this composition. The pure glass powder only crystallized from 750°C. The Nb_2O_5 favors the formation of crystalline structures in the vitreous matrix at low temperatures and with piezoelectric structures.

1. Introduction

Because the consumption habits of the population have generated environmental problems such as the growth of landfills and depletion of natural resources [1, 2], scientific research has been much requested regarding the recycling of discarded materials, for finding new utilities and generating value from the waste [2–5]. Glass, despite being recyclable, occupies large volumes in landfills [6]. Considering the scope of the windshields, 40 million vehicles in the world reach the end of life every year [1] and throughout the useful life of vehicles, they may be changed and discarded. In addition, the windshields are more laborious to recycle. This is due to the PVB (polyvinyl butyral) film, which exists between layers of glass, whose function is to protect the occupants, preventing the glass from shattering when breaking on impact [7]. Several studies have proposed the use of glass for the production of glass-ceramics, adding value and targeting a discarded material [2, 8–10].

The silicates, which are the basis of the glasses, can be used for the production of profitable products such as glass-ceramics [2]. When compared to glass, it has greater stability, durability, superior mechanical properties, resistance to thermal shock, low coefficients of thermal expansion, and fracture toughness [11, 12]. It features a range of applications, including the manufacture of artificial bones and teeth, heat shock-resistant transparent pans, heat-resistant windows for stoves or ovens, building walls, and cooktops [13–15]. There is a considerable amount of research focused on the production of glass-ceramics with industrial waste [2, 10, 16–19]. The work of Lu et al. may be highlighted, which studied the influence of sintering and crystallization on the mechanical properties of glass-ceramics produced by glass and fly ash from thermal power plants.

The addition of a nucleating agent to the glass powder is used to induce volumetric crystallization and reduce crystallization temperatures. The nature of crystallinity and the distribution of the crystalline phase formed during crystallization are dependent on the type and amount of the nucleating agent used. The presence of nucleating agents, such as TiO_2 and various oxides, in the glass-ceramic composition favors nucleation and crystal growth. Since the surface tension decreases, the nucleation rate increases in the vitreous system [13, 20, 21]. The addition of niobium oxide in addition to promoting crystallization also enables the formation of crystals of the perovskite group. The piezoelectric properties exhibited by perovskite glass-ceramics have been extensively studied [22].

In this work, glass-ceramics were produced from discarded glass with properties compatible with those found in the literature for this material. The produced glass-ceramics were studied in terms of their flexural strength, mass density, crystallinity, microstructure formation, and biocompatibility for medical applications. In addition, this work also investigated the chemical composition and statically measured the particle sizes of the raw material produced before the sinterization procedure.

2. Methodology

The experimental and characterization methodologies followed in this work are presented. The production of the glass powder and the obtaining of the glass-ceramics are detailed. According to each experimental step, the procedures associated with the adopted characterization techniques are presented.

2.1. Production and Characterization of Glass Powder. Windshield slices, glass blade, and PVB were milled and separated in a ball mill. The glass powder was passed through a 65-mesh sieve. The granulometric distribution was measured (Mastersizer Hydro 2000MU, Malver, United Kingdom), and the chemical elements of the glass powder were quantified by X-ray fluorescence (S8 Tiger Spectrometer, Bruker X-ray, United States).

2.2. Production and Characterization of the Specimens. The glass powder was mixed with 10% water by weight, introduced in a rectangular metal matrix (28.31 mm length × 7.30 mm wide), and a 11.59 MPa load was applied with a hydraulic press for one minute (P10 ST 10 ton, Bovenau, Brazil). The specimens were extracted from the matrix and dried at 110°C for one hour (400/3ND, Nova Ética, Brazil). They were then heated at 5°C/min rate and sintered for one hour at 600, 650, 700, 750 and 800°C temperatures. Some specimens were produced with the addition of 4% of niobium oxide during the mix process under the same conditions.

Groups 1, 2, and 3 are the glass powder (GP) specimens sintered at temperatures of 650, 700, and 750°C, respectively. Groups 4, 5, and 6 are the glass powder and niobium oxide (GPN) specimens sintered at temperatures of 650, 700, and 750°C, respectively. Group 7 is a GPN composition specimen sintered at 600°C, while Group 8 is a GP specimen sintered at 800°C.

The thermodifferential and thermogravimetric analyses (Simultaneous Thermal Analyzer STA 6000, PerkinElmer, United States) were carried out on specimens in an air atmosphere with a heating rate of 5°C/min and a temperature range between 30 and 900°C. The densities were determined by the Archimedes method, according to standard NBR 6220:2011 [23].

The flexural tests were performed at three points according to ASTM C1161-13 [24] in thirteen specimens from each group with thickness from 2.23 to 3.96 mm. The distance between the supports was 20 mm, and the loading rate was 0.2 mm/min (Shimadzu AGX-PLUS, Japan). The reliability of the flexural strength results was determined by the Weibull method [25]. Scanning electron microscopy (SEM) was performed on each group on a fracture surface (UltraDry EDS JEOL JSM6510LV, Thermo Fisher Scientific, United States).

X-ray diffraction (XRD) analysis was performed (Bruker-D8 Endeavor diffractometer, United States) on each group after ground on CuKa 40 kV/40 mA parameters. The scan range of diffractogram was 4–80° with a scan speed of 0.02°·2°/2 s. The qualitative spectrum interpretations were performed by comparison with standards contained in the PDF02 database (ICDD, 2006) in Bruker Diffrac Plus software.

For in vitro static biofilm tests, the overnight culture of a multivirulent methicillin resistant wild-type strain (USA300) was diluted 1 : 100 in TSB supplemented with 0.5% glucose (TSB-G). Diluted bacteria were mixed with 20% pooled human plasma and used for assessment of biofilm formation on fragments of rat mandible (CEUA 740), commercial bone grafts (Aloboneporos–Osseocon 1.0 g, Clonos Dental, Lumina Bone-Criteria Biomaterials, Brazil), and Groups 1–8.

The specimens were fixed to the bottom of a 12-well polystyrene plate with Lubriseal grease (Thomas Scientific, United States) and sterilized by ultraviolet irradiation. Multiwell plates were incubated at 37°C with shaking at 100 rpm for one hour and then further incubated at 37°C without shaking for 24 h. The wells were washed three times

with phosphate buffered saline to remove nonadherent cells. Adherent biofilms were fixed with methanol, stained with crystal violet and washed three times with sterile water. Biofilm biomass formed on the mandible, bone grafts, and specimens from Groups 1–8 was determined by solubilizing crystal violet with 33% acetic acid [26] and measured at 490 nm light wavelength using a microtiter plate reader (Biorad, United States). All biofilm biomass experiments were performed in triplicates.

The unpaired Student's t-test with the Tukey multiple comparison post hoc test was used to assess the statistical significance of between-group differences in bacterial count in vitro biofilm biomass with 95% confidence interval ($p < 0.05$).

3. Results and Discussion

The granulometric distribution of the glass powder resulted in a monomodal distribution with d (10) of 2.001 μm, d (50) of 14.658 μm, and d (90) 57.234 μm. Cho and Kim [11] separated three particle average sizes for the production of glass-ceramics. It was observed that the smaller particle size favors densification, especially in the lower sintering temperatures. These smaller particles favored the coalescence process during the sintering. In this study, the mean particle size was higher than the average particle size of Cho and Kim [11].

Table 1 shows the result of X-ray fluorescence spectroscopy of the glass powder. It is noted that the glass powder is composed primarily of silicon oxide, with about 80% by weight of the total composition. Sodium, calcium, and magnesium oxides are present in the composition at much lower levels. Aluminum oxide comprises the lowest content in the composition.

Figure 1 shows the differential thermal analysis (DTA), thermogravimetric analysis (TG), and derivative thermogravimetric analysis (DTG). A peak is observed in DTA between 700°C and 800°C for GP and GPN groups. This peak is not associated with mass loss, as can be seen in DTG. It indicates physical phenomena in the temperature range between 600°C and 900°C. Any variation was observed with the amount of niobium oxide added to the glass powder, even though it is considered a nucleating agent. In these analyses, important parameters can be obtained for the production of glass-ceramics, such as the glass transition temperature (t_g) and the crystallization temperature (t_c) of the glass powder. The nucleation of the crystals in the glass matrix will only occur in temperatures higher than the glass transition temperature. The t_g is found when a slight endothermic depression begins, followed by a strong release of heat, corresponding to the crystallization peak of the differential thermal analysis (DTA).

Figure 2 shows the X-ray diffractogram of the GP and GPN specimens. In the samples with only glass powder, produced in the temperatures of 650°C and 700°C, the structure remains totally amorphous. At the temperature of 750°C, some peaks began to form already, with imperfect crystalline structures, indicating the presence of crystals of albite, quartz, and diopsite. The addition of niobium oxide favored the formation of crystalline structures, confirming the production of glass-ceramics at temperatures of 650, 700, and 750°C (Figure 2). The peak intensities of zeolite and stilbite were lower than those of isolueshite crystal structure, which is a sodium niobate, $NaNbO_3$.

Table 1: Composition and concentration of pure glass powder.

Composition	SiO_2	Na_2O	CaO	MgO	Al_2O_3
Percentage (%)	80.10	8.86	7.97	2.34	0.75

The burning temperatures used are higher than those used for the synthesis of sodium niobate by solid reaction of niobium oxide and sodium hydroxide [26]. It is important to note that all the crystalline structures have chemical elements coherent with those found in X-ray fluorescence. Given these results, two other groups were made and added to be studied. The possibility of producing glass-ceramics at different sintering temperatures according to the composition on the specimens was considered. Hence, one group consists of GPN specimens sintered at 600°C (Group 7) and the other of GP specimens sintered at 800°C (Group 8). Table 2 and Figure 3 show the mean density value for each group. The GP specimens showed a decrease in the mass density, with the sintering temperature increasing up to 750°C. After this value, there is no significant change in the density of the specimens with increasing temperature, as can be observed in Figure 3, from the densities obtained through sintering at 750°C and 800°C. When crystallization occurs before completion of the sintering, the viscous flow viscosity increases rapidly and prevents the sintering process resulting in less dense materials [27]. This occurred at the temperatures 750°C and 800°C, where the crystallization of the glass powder occurred before completed sintering.

The GPN specimens showed density values between 2,115 and 2,339 g/cm^3. Increasing the sintering temperature from 600°C to 650°C resulted in increased density due to coalescence of the particles. However, at 700°C, the density decreases due to the better crystallization of the stilbite, which causes a reduction of sintering by viscous flow, making the densification difficult. After 700°C, the density is maintained in a close value when the sintering temperature increased to 750°C, with the formation of a new crystalline structure, albite, occurring.

At the sintering temperature of 650°C, it can be observed that the density was higher for the GP specimens. There was crystallization of the specimens with the addition of niobium oxide at 650°C, rapidly increasing the viscosity, preventing the sintering, and producing less dense specimens. No crystalline phase formation occurred in the GP specimens at 650°C, which favored sintering and densification.

The fracture surface of the GP specimens is presented in Figure 4. It is possible to observe that there is an increase in the number and size of the pores with the increasing sintering temperature, justifying the density decrease. The size of the pores seems smaller and more homogeneous in the GPN specimens (Figure 5).

The mean flexural strength at different sintering temperatures is shown in Table 3 and in Figure 6. These results

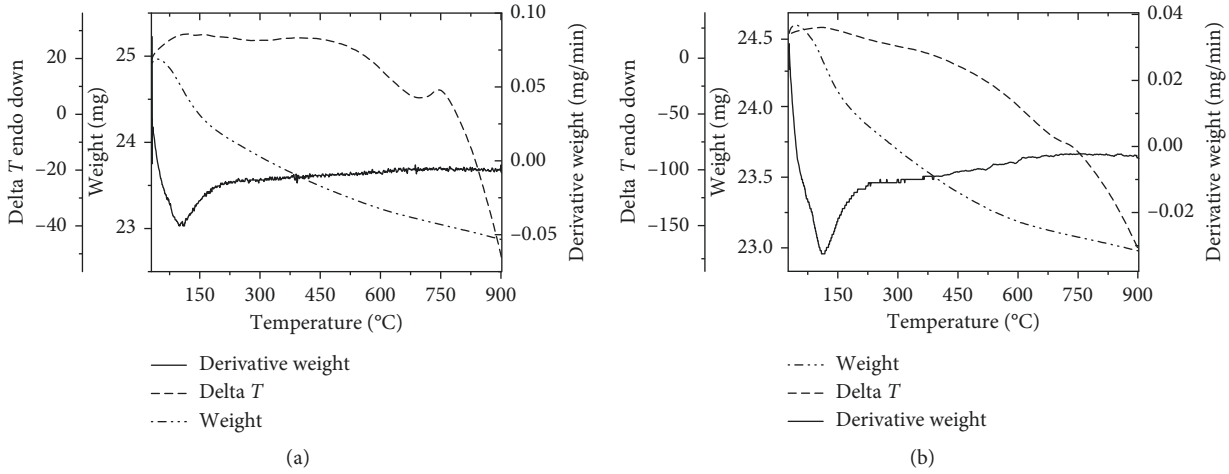

Figure 1: Thermal analysis of the (a) OGP group and (b) GPN group using DTA, TG, and DTG.

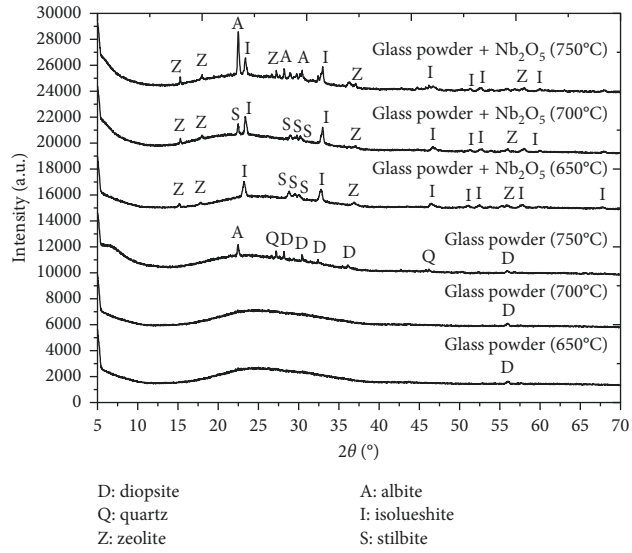

Figure 2: X-ray diffractogram of Groups 1–6.

Table 2: Average density and standard deviation of the groups.

Group	Composition	Sintering temperature (°C)	Average density (g/cm^3)	Standard deviation (g/cm^3)
1	Glass powder	650	2.433	0.157
2	Glass powder	700	2.216	0.273
3	Glass powder	750	2.091	0.130
4	Glass powder + Nb_2O_5	650	2.339	0.148
5	Glass powder + Nb_2O_5	700	2.219	0.219
6	Glass powder + Nb_2O_5	750	2.173	0.028
7	Glass powder + Nb_2O_5	600	2.115	0.180
8	Glass powder	800	2.060	0.057

showed that the niobium oxide decreases the flexural strength of specimens, comparing the results of the GPN and GP groups. Despite this, the results are satisfactory since the obtained flexural strengths are within the usual values for glass-ceramics [28].

Cho and Kim [11] obtained an average of 84.00 MPa for the flexural strength of the sintered specimens at a temperature of 900°C, when the largest mean particle size used was 4.8 μm. In this text, glass powder particles with a wide range of granulometric distribution were used, with similar results, 77.64 MPa, in lower sintering temperatures. The similar mechanical properties were obtained due to the use of the wide-ranged granulometric normal distribution instead of the separation in narrow bands of particle sizes. In

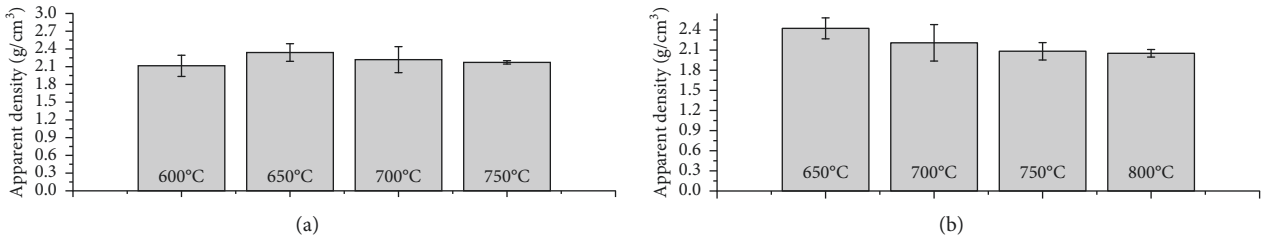

Figure 3: Variation of the density with the sintering temperature.

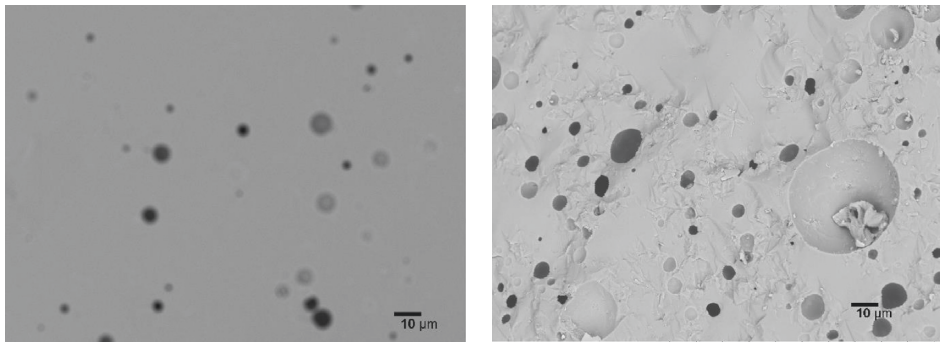

Figure 4: SEM of OGP: (a) Group 2 and (b) Group 3.

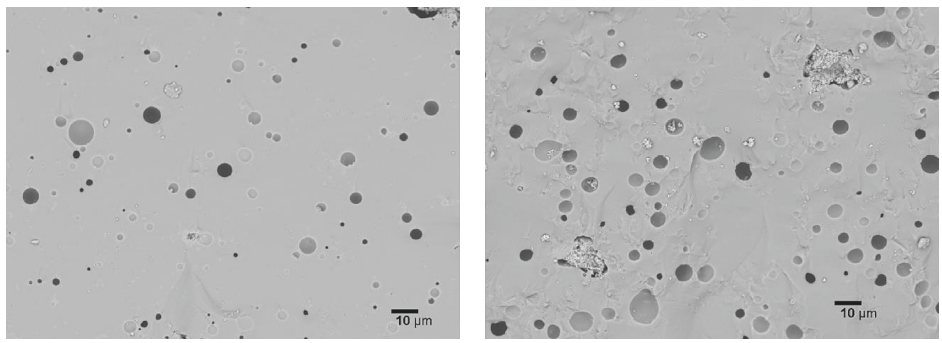

Figure 5: SEM of GPN: (a) Group 5 and (b) SE Group 6.

Table 3: Flexural strength and Weibull modulus of all groups.

Group	Flexural strength (MPa)	Standard deviation (MPa)	Weibull modulus (m)	R^2
1	74.67	21.09	2.50	0.83
2	77.64	14.54	5.41	0.81
3	52.47	7.06	6.87	0.93
4	43.86	5.85	7.42	0.86
5	38.25	6.81	5.66	0.94
6	40.10	6.71	5.96	0.93
7	29.15	5.41	5.15	0.92
8	52.57	6.47	8.03	0.96

this case, the adopted methodology may have facilitated the compaction factor of the shaped specimens and thereby have improved the densification, justifying the similarity of the results.

Since crystallization influences the densification of the material, it also influences the strength of the material because both the internal and external porosity act as stress concentrators. Thus, the bulk crystallization promoted by

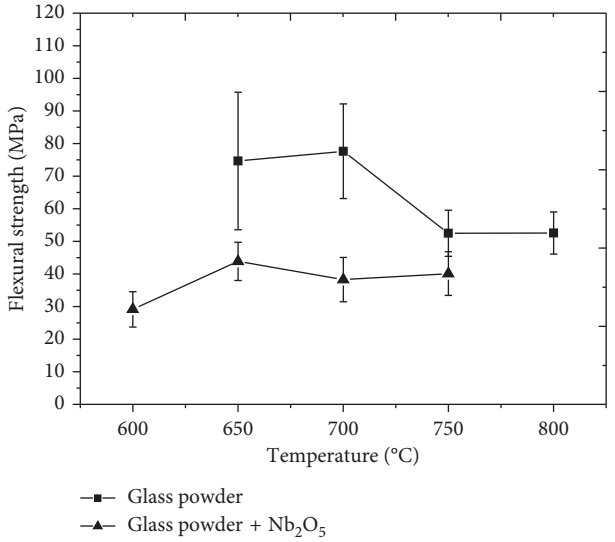

Figure 6: Flexural strength of all groups.

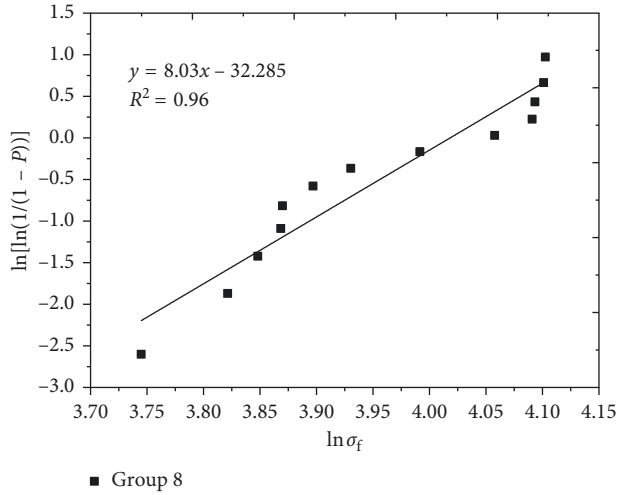

Figure 7: Graph with data associated with Weibull parameters for Group 4.

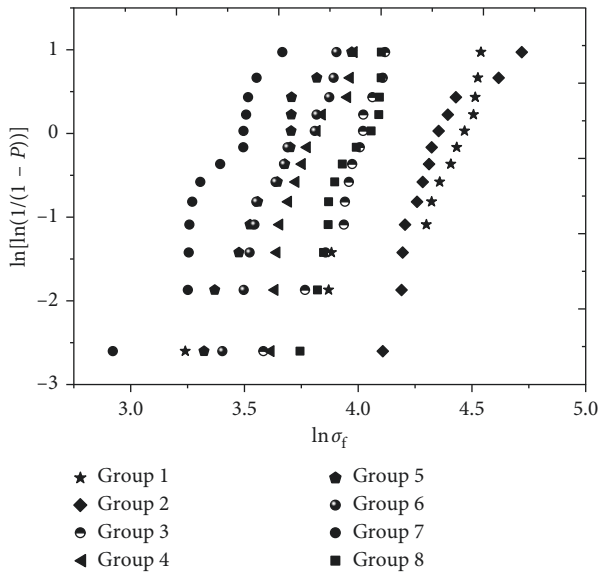

Figure 8: Graph with data associated with Weibull parameters for all groups.

niobium oxide increases the viscosity that prevents the exit of gases making the material porous [29]. On the other hand, the presence of niobium oxide promotes the formation of isolueshite, the structure with piezoelectric properties and high dielectric constant. Therefore, despite the reduction of resistance, the existence of isolueshite allows for the exploration of electrical applications of glass-ceramics [30, 31].

Zhang and Liu [8] also realized that crystallization increases viscosity and hinders densification. In addition, it was observed that, in higher temperatures, the surface densification is improved, because resistance of the viscous flow of the glass is smaller on the surface than in the interior part. This is a fact that favors mechanical resistance. In the glass-ceramics of this work, the improvement of the mechanical properties, provided by the surface densification, is not perceived since the internal porosity is increased with the increase of temperature.

The Weibull modulus (m) was determined to evaluate the reliability of the flexural strength results (Table 3). Figure 7 shows the slope of the line which was used to determine the Weibull modulus, obtained from the results of flexural strength of the thirteen specimens. In this case, the specimens were sintered at the temperature of 800°C and the composition was glass powder. The acceptable range of the Weibull parameter, m, is between 3 and 15 for fragile materials [25], but Group 1 was not satisfactory. The higher the value of m, the more reliable is the results of the mechanical properties [32] (Figure 8). The correlation factors, R^2, presented in Table 2, were higher than 0.800, which can be considered as satisfactory [33].

The in vitro biofilm formed on the mandible was reduced when compared to the biomass biofilm formed on commercial bone grafts. Glass-ceramics Groups 1–8 showed less biofilm formation ($^*p = 0.0477$) when compared to mandible bone, indicating that these groups of glass-ceramics severely attenuated *Staphylococcus aureus* attachment. These results suggest that these glass-ceramics were biocompatible and can be used as dental prostheses (Figure 9).

4. Conclusions

The monomodal distribution contributed to obtaining better mechanical properties at lower temperatures compatible with those in the literature, even with a larger average particle size. The recycled glass powder of windshield presented chemical composition like other glass-ceramics produced with raw material of greater cost. Thermal analyses showed crystallization temperatures close to 700°C in the two compositions. The addition of niobium oxide favored the formation of crystals at the temperatures at which sintering occurred. On the other hand, it made it difficult to densify specimens at lower temperatures. However, pure glass powder favors densification at lower temperatures and higher porosity at higher temperatures. The addition of niobium oxide decreased the flexural strength compared to

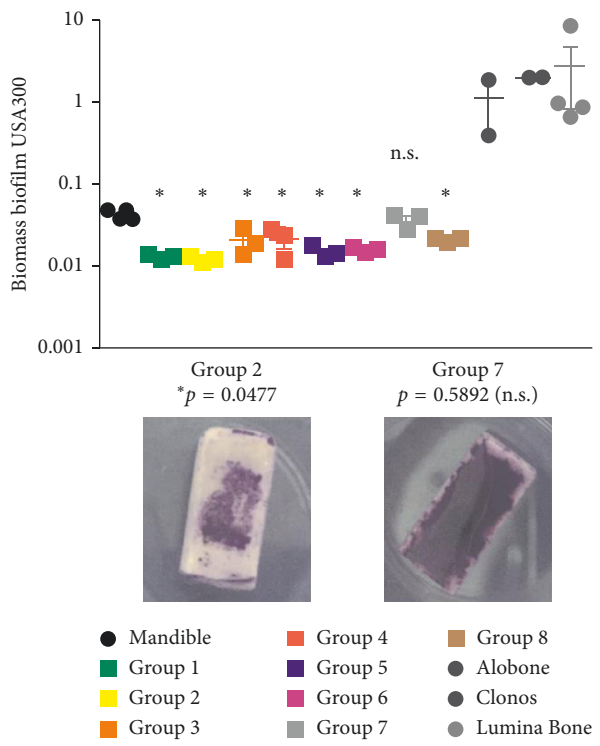

Figure 9: Biomass quantification of *Staphylococcus aureus* (USA300) biofilm formed on glass-ceramics, mandible, and bone grafts. Representative images of biofilms after staining with crystal violet are shown at the bottom of *x*-axis (Group 2 × Group 7).

pure glass powder specimens. Even so, such results agree with the literature. The glass-ceramics produced in this work presented smaller biomass formation than the mandible and bone grafts, suggesting a possible application for dental prostheses and oral rehabilitation, after performing other tests for biocompatibility.

Data Availability

The data used to support the findings of this study are available from the corresponding author upon request.

Conflicts of Interest

The authors declare that there are no conflicts of interest regarding the publication of this paper.

Acknowledgments

The authors are grateful for the financial support of FAPERJ, CAPES, and CNPq, as well as the Center for Mineral Technology, CETEM, for the use of MEV and X-ray diffractometer and the National Institute of Technology, INT, for X-ray fluorescence analysis.

References

[1] F. O. Marques and L. A. Meirelles, *Tendências da Reciclagem de Materiais na Indústria Automobilística*, CETEM/MCT, Rio de Janeiro, Brazill, 2007.

[2] J. Lu, X. Cong, and Z. Lu, "Influence of magnesia on sinter-crystallization, phase composition and flexural strength of sintered glass-ceramics from waste materials," *Materials Chemistry and Physics*, vol. 174, pp. 143–149, 2016.

[3] M. Mayyas, F. Pahlevani, W. Handoko et al., "Preliminary investigation on the thermal conversion of automotive shredder residue into value-added products: graphitic carbon and nano-ceramics," *Waste Management*, vol. 50, pp. 173–183, 2016.

[4] E. Barrachina, M. Esquinas, J. Llop, M. D. Notari, and J. B. Carda, "Development of a glass-ceramic glaze formulated from industrial residues to improve the mechanical properties of the porcelain stoneware tiles," *Materials Letters*, vol. 220, pp. 226–228, 2018.

[5] H. Mi, J. Yang, Z. Su et al., "Preparation of ultra-light ceramic foams from waste glass and fly ash," *Advances in Applied Ceramics*, vol. 116, no. 7, pp. 400–408, 2017.

[6] T. C. Ling, C. S. Poon, and H. W. Wong, "Management and recycling of waste glass in concrete products: current situations in Hong Kong," *Resources, Conservation and Recycling*, vol. 70, pp. 25–31, 2013.

[7] K. C. Ahn, "The dynamic effect of PVB interlayer thinkness on laminated glass window," *IJET: International Journal of Engineering and Technology*, vol. 15, no. 5, pp. 33–40, 2015.

[8] W. Zhang and H. Liu, "A low cost route for fabrication of wollastonite glass–ceramics directly using soda-lime waste glass by reactive crystallization–sintering," *Ceramics International*, vol. 39, no. 2, pp. 1943–1949, 2013.

[9] C. S. Fan and K. C. Li, "Production of insulating glass ceramics from thin film transistor-liquid crystal display (TFT-LCD) waste glass and calcium fluoride sludge," *Journal of Cleaner Production*, vol. 57, pp. 335–341, 2013.

[10] J. Cao, J. Lu, L. Jiang, L. Jiang, and Z. Jiang, "Sinterability, Microstructure and compressive strength of porous glass ceramics from metallurgical silicon slag and waste glass," *Ceramics International*, vol. 42, no. 8, pp. 10079–10084, 2016.

[11] I. S. Cho and D. Kim, "Glass-frit size dependence of densification behavior and mechanical properties of zinc aluminum calcium borosilicate glass-ceramics," *Journal of Alloys and Compounds*, vol. 686, pp. 95–100, 2016.

[12] X. Wang, L. Wu, H. Li, J. Xiao, X. Cai, and Y. Teng, "Preparation and characterization of SO_3-doped barium borosilicate glass ceramics containing zirconolite and barite phases," *Ceramics International*, vol. 43, no. 1, pp. 534–539, 2017.

[13] K. Maeda, Y. Sera, and A. Yasumori, "Effect of molybdenum and titanium oxides on mechanical and thermal properties of cordierite–enstatite glass-ceramics," *Journal of Non-Crystalline Solids*, vol. 434, pp. 13–22, 2016.

[14] W. Höland, V. Rheinberger, E. Apel, and C. van't Hoen, "Principles and phenomena of bioengineering with glass-ceramics for dental restoration," *Journal of the European Ceramic Society*, vol. 27, no. 2-3, pp. 1521–1526, 2007.

[15] C. Ritzberger, M. Schweiger, and W. Höland, "Principles of crystal phase formation in Ivoclar Vivadent glass-ceramics for dental restorations," *Journal of Non-Crystalline Solids*, vol. 432, pp. 137–142, 2015.

[16] J. Kang, J. Wang, J. Cheng, J. Yuan, Y. Hou, and S. Qian, "Crystallization behavior and properties of CaO-MgO-Al_2O_3-SiO_2 glass-ceramics synthesized from granite wastes," *Journal of Non-Crystalline Solids*, vol. 457, pp. 111–115, 2017.

[17] I. Rozenstrauha, E. Lodins, L. Krage et al., "Functional properties of glass–ceramic composites containing industrial inorganic waste and evaluation of their biological compatibility," *Ceramics International*, vol. 39, no. 7, pp. 8007–8014, 2013.

[18] M. Tarrago, M. Garcia-Valles, M. H. Aly, and S. Martínez, "Valorization of sludge from a wastewater treatment plant by glass-ceramic production," *Ceramics International*, vol. 43, no. 1, pp. 930–937, 2017.

[19] X. Lu, Y. Li, W. Dai, and D. Cang, "Effect of composition and sintering process on mechanical properties of glass ceramics from solid waste," *Advances in Applied Ceramics*, vol. 115, no. 1, pp. 13–20, 2016.

[20] D. P. Mukherjee and S. K. Das, "The influence of TiO_2 content on the properties of glass ceramics: crystallization, microstructure and hardness," *Ceramics International*, vol. 40, no. 3, pp. 4127–4134, 2014.

[21] Y. Sakai, T. Futakuchi, T. Karaki, and M. Adachi, "Effects of NiO addition on (K,Na,Li)NbO_3–$BaZrO_3$–(Bi,Na)TiO_3-based ceramics," *Japanese Journal of Applied Physics*, vol. 53, no. 9S, article 09PB07, 2014.

[22] D. F. Han, Q. M. Zhang, J. Luo, Q. Tang, and J. Du, "Glass-ceramic nanocomposites in the [(1−x) PbO–xBaO]–Na_2O–Nb_2O_5–SiO_2 system: crystallization and dielectric performance," *Solid State Sciences*, vol. 14, no. 6, pp. 661–667, 2012.

[23] Associação Brasileira de Normas Técnicas (ABNT). NBR 6220, *Dense refractory Material-Determination of Bulk Density, Apparent Porosity, Absorption and Bulk Density of the Solid Part*, ABNT, Rio de Janeiro, Brazil, 2011.

[24] American Society for Testing and Materials (ASTM), "C1161–13: standard test method for flexural strength of advanced ceramics at ambient temperature," in *Annual Book of ASTM*, 2013, Standards No. 309–315.

[25] A. R. Migliore Júnior and E. D. Zanotto, "Sobre a determinação dos parâmetros de Weibull (On the determination of Weibull parameters)," *Cerâmica*, vol. 38, p. 253, 1992.

[26] L. M. S. Azevedo, "Synthesis of sodium niobate from niobium oxide and metallic niobium," Thesis, Instituto Militar de Engenharia, Rio de Janeiro, Brazil, 2010.

[27] C. Fredericci, H. N. Yoshimura, A. L. Molisani, M. M. Pinto, and P. F. Cesar, "Effect of temperature and heating rate on the sintering of leucite-based dental porcelains," *Ceramics International*, vol. 37, no. 3, pp. 1073–1078, 2011.

[28] J. Yang, S. Zhang, B. Liu, D. Pan, C. Wu, and A. A. Volinsky, "Effect of TiO_2 on crystallization, microstructure and mechanical properties of glass-ceramics," *Journal of Iron and Steel Research International*, vol. 22, no. 12, pp. 1113–1117, 2015.

[29] P. Alizadeh and V. K. Marghussian, "Effect of nucleating agents on the crystallization behaviour and microstructure of SiO_2–CaO–MgO (Na_2O) glass-ceramics," *Journal of the European Ceramic Society*, vol. 20, no. 6, pp. 775–782, 2000.

[30] T. Zeng, X. L. Dong, C. L. Mao, Z. Y. Zhou, and H. Yang, "Effects of pore shape and porosity on the properties of porous PZT 95/5 ceramics," *Journal of the European Ceramic Society*, vol. 27, no. 4, pp. 2025–2029, 2007.

[31] K. Singh, V. Lingwal, S. C. Bhatt, N. S. Panwar, and B. S. Semwal, "Dielectric properties of potassium sodium niobate mixed system," *Materials Research Bulletin*, vol. 36, no. 13-14, pp. 2365–2374, 2001.

[32] X. Fan, E. D. Case, I. Gheorghita, and M. J. Baumann, "Weibull modulus and fracture strength of highly porous hydroxyapatite," *Journal of the Mechanical Behavior of Biomedical Materials*, vol. 20, pp. 283–295, 2013.

[33] B. Defez, G. Peris-Fajarnés, V. Santiago, J. M. Soria, and E. Lluna, "Influence of the load application rate and the statistical model for brittle failure on the bending strength of extruded ceramic tiles," *Ceramics International*, vol. 39, no. 3, pp. 3329–3335, 2013.